Neutron total cross section measurements of gold and tantalum at the nELBE photoneutron source[1]

Roland Hannaske, Zoltan Elekes, Roland Beyer, Arnd Junghans[2], Daniel Bemmerer, Evert Birgersson[3], Anna Ferrari, Eckart Grosse*, Mathias Kempe*, Toni Kögler*, Michele Marta[4], Ralph Massarczyk*, Andrija Matic[5], Georg Schramm*, Ronald Schwengner, and Andreas Wagner*
Helmholtz-Zentrum Dresden-Rossendorf, Bautzner Landstr. 400, 01328 Dresden, Germany

Abstract
Neutron total cross sections of ^{197}Au and ^{nat}Ta have been measured at the nELBE photoneutron source in the energy range from 0.1 - 10 MeV with a statistical uncertainty of up to 2 % and a total systematic uncertainty of 1 %. This facility is optimized for the fast neutron energy range and combines an excellent time structure of the neutron pulses (electron bunch width 5 ps) with a short flight path of 7 m. Because of the low instantaneous neutron flux transmission measurements of neutron total cross sections are possible, that exhibit very different beam and background conditions than found at other neutron sources.

1 Introduction

Experimental neutron total cross sections as a function of neutron energy are a fundamental data set for the evaluation of nuclear data libraries. With increasing neutron energy the compound nucleus resonances cannot be resolved anymore and will start to overlap. In the energy range of fast neutrons, which is especially important for innovative nuclear applications, like accelerator driven systems for the transmutation of nuclear waste, the neutron total cross section can be described by optical model calculations (e.g. [2, 3]) where the range below 5 MeV shows a large sensitivity on the optical model parameters.

The neutron total cross section of ^{197}Au in the energy range from 5 – 200 keV is an item in the OECD NEA Nuclear Data High Priority Request list as ^{197}Au(n,γ) is an activation standard in dosimetric applications [4]. Precise total cross section data with a targeted uncertainty < 5 % will have a direct impact on future evaluations of neutron induced reactions on Au. Also an overlapping measurement from 200 keV to 2.5 MeV is of interest to check consistency.

Tantalum is a non-corrosive metal of importance as a structural material in many nuclear and high-temperature applications, e.g. it is also a component in Reduced Activation Ferritic / Martensitic steels [5]. The fast neutron cross section of tantalum has been evaluated recently [6]. In that work, a careful measurement of the neutron total cross section from several tens of keV to several MeV with an accuracy goal of ≈ 1 % has been recommended.

---

[1] This article is an updated and abridged version of Ref. [1].

* also at Technische Universität Dresden, Dresden, Germany

[2] Corresponding author: Tel. +49 351 260 3589; email: a.junghans@hzdr.de

[3] Present address: AREVA NP GmbH, 91052 Erlangen, Germany

[4] Present address: GSI Helmholtzzentrum für Schwerionenforschung GmbH, Planckstr. 1, 64291 Darmstadt, Germany

[5] Present address: IBA Particle Therapy, 45157 Essen, Germany

A comprehensive set of very precise high energy neutron total cross sections up to several hundred MeV neutron energy has previously been measured at the Weapons Neutron Research (WNR) spallation neutron source of the Los Alamos National Laboratory (LANL) [7, 8]. Due to experimental constraints these data start at 5 MeV neutron energy, but are still valuable to compare to. At lower energies precise measurements exist using neutrons from the ^{7}Li(p,n)^{7}Be reaction at the Fast Neutron Generator of Argonne National Laboratory (ANL) [9]. Neutron total cross sections of ^{197}Au in the energy region from 4 to 108 keV have been measured recently at the GELINA facility [10]. These data are complemented by the work reported here using a neutron source with very different beam and background properties.

The neutron total cross sections for tantalum of natural isotopic composition (99.95 % purity) and ^{197}Au (99.99 % purity) were determined by the transmission technique at the photoneutron source nELBE [11–13] at Helmholtz-Zentrum Dresden-Rossendorf, Germany. This is the world's only neutron time-of-flight facility driven by a superconducting electron accelerator [14] with its superior time structure definition. The very short (5 ps) electron bunches allow us to use a short flight path (7.175 m) with a good time resolution and maximize the available neutron intensity with a high repetition rate in continuous-wave (cw) operation (101.5625 kHz micropulse repetition rate). This rate is two to three orders of magnitude higher than the pulsed operation at normal-conducting accelerators. A fast plastic scintillator with low detection threshold [15] was used for the time-of-flight measurements. The neutron spectrum of this facility is characterized in a separate publication [12]. The energy range extends from ≈ 10 keV to 10 MeV, which essentially covers the fission neutron spectrum.

First we shortly describe the nELBE neutron time-of-flight facility and the setup for transmission measurements and then we present the data analysis and discuss the results.

2 The nELBE time-of-flight facility

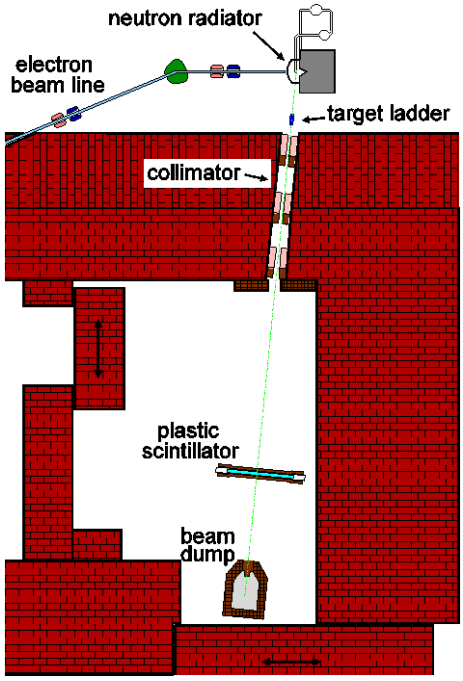

Fig. 1: Floor plan of the cave for the neutron transmission experiment at the ELBE accelerator. The neutron radiator consists of a Mo tube with rhombic cross section through which liquid lead is flowing. The target ladder is located approx. 1 m from the neutron radiator in front of the collimator tube which has a length of

2.6 m. The total flight path to the neutron detector (plastic scintillator) is 7.175 m. A beam dump behind the plastic scintillator absorbs the bremsstrahlung and neutrons.

At Helmholtz-Zentrum Dresden-Rossendorf the world's only compact photoneutron source at a superconducting electron accelerator dedicated to measurements in the fast neutron range has been built. A compact liquid lead circuit is used as a neutron-producing target. Through this technology the neutron beam intensity is not limited by the heat dissipation inside the target. The technical design including thermo-mechanical parameters of the liquid lead circuit and the beam dump is discussed in Ref. [13]. The electron beam is accelerated to 30 MeV in cw-mode by superconducting cavities. The maximum average beam current at a micropulse rate of 13 MHz is 1 mA. The neutron source strength at the nominal beam current has been calculated with the Monte Carlo N-Particle Transport Code MCNP-4C3 to be 10^{13} neutrons/s [11]. The accelerator produces high brilliance beams with variable micropulse repetition rates and duty cycles. The bunch duration is about 5 ps, so that the time-of-flight resolution is not degraded and short flight paths can be used with a high-resolution detection system.

Figure 1 shows the floor plan of the neutron time-of-flight facility. The electron beam passes through a beryllium window mounted on a stainless-steel vacuum chamber and hits the radiator, consisting of a molybdenum channel confining the liquid lead. The channel has a rhombic cross section with 11 mm side length. The electrons generate bremsstrahlung photons which release neutrons in secondary (γ,n) reactions on lead. These leave the radiator almost isotropically, whereas the angular distributions of electrons and photons are strongly forward-peaked. The collimator axis is located at 95° with respect to the electron beam direction. The collimator and the neutron beam properties at the experimental area have been optimized using MCNP-4C3 in order to maintain the correlation of time-of-flight and neutron energy [11]. The collimator of 2.6 m length contains three replaceable elements of lead and borated polyethylene that are mounted inside a precision steel tube [11].

3 Transmission

The neutron total cross sections were determined in a transmission experiment. The target samples together with bremsstrahlung absorbers were mounted in a pneumatically driven computer-controlled target ladder directly in front of the collimator entrance. The conical neutron beam collimator has an entrance aperture diameter of 20 mm increasing to 30 mm at the exit. In this geometry small diameter samples were used with a neutron transmission factor of about 0.5. The target samples were periodically moved in and out of the beam to compensate for possible long term drifts in the neutron beam intensity. The data taking time per cycle for the empty sample (3 cm thick Pb bremsstrahlung absorber only) was 600 s, for the Au and Ta samples it was 900 s. The total measurement time was about 78 hours. The order of the cycle was empty-Au-Ta-Pb in the first half of the experiment whereas it was empty-Au-empty-Ta-empty-Pb in the second half with 300 s duration for empty, to increase the frequency of empty target measurements. Each sample was combined with a 3 cm thick Pb absorber to reduce the bremsstrahlung count rate. All Pb absorbers and the Pb sample were made from a technical lead alloy (PbSb4). The data from the Pb sample have been used to determine the energy resolution of the time-of-flight measurement.

The transmitted neutrons were detected using a plastic scintillator (Eljen EJ-200, 1000 mm x 42 mm x 11 mm) that was read out on both ends using high-gain Hamamatsu R2059-01 photomultiplier tubes (PMT). The scintillator is surrounded by a 1 cm thick lead shield to reduce the background count rate. The detection threshold for recoil protons in this detector is at about 10 keV [15]. The overlap neutron energy for the given micropulse repetition rate and flight path is 2.8 keV. This is below the detection threshold of the plastic scintillator used in the transmission measurement. The electron beam intensity was reduced to the sub μA range to have a detector

count rate of ≈ 10 kHz (empty sample beam). This corresponds to a neutron count rate of ≈ 250 n/s. On average, only every tenth accelerator bunch is registered by the scintillator.

The time-of-flight of the transmitted neutrons was measured in list mode with the Multi-Branch-System (MBS) real-time data acquisition developed at GSI, Darmstadt. This setup is optimized to control several VME bus crates with several front-end processors using a real-time operating system. The PMT output signals were fed into a CAEN V874B 4 Channel BaF_2-Calorimeter Read-Out Unit housing charge to digital converter (QDC) and constant fraction discriminator (CFD) sections. An internal constant veto time of ≈ 2.7 µs in this module helps to suppress the rate of afterpulses that may occur in high-gain PMTs. The CFD output signals were fed into a SIS 3820 scaler module to determine the detector count rate and into the multi-hit multi-event time-to-digital converter (TDC) CAEN V1190A to determine the time information with a dispersion of 97.6 ps/channel. The accelerator radiofrequency (rf)-signal serves as reference for the time-of-flight determination. A CAEN V1495 FPGA module was used to produce the logical AND of the CFD signals from both PMTs to trigger the data acquisition (DAQ). The coincident signals from the TDC that triggered the data acquisition were analysed for this transmission measurement. The time sum signal of both PMTs is used to measure the time-of-flight, while a software condition on the time difference signal was used to select events that occurred in the central beam spot region of the scintillator bar. The absolute scale of time-of-flight is determined using the bremsstrahlung peak and the known flight path. The flight path has been verified by resonant structures that appear in the neutron spectrum [12]: Several absorption minima appear due to resonances with strong elastic neutron scattering in ^{208}Pb. Emission peaks appear in the neutron spectrum from nuclear levels just above the neutron separation energy mainly in ^{208}Pb that can be excited via (γ,n) or (e,e'n) reactions.

The transmission *T* is given by the relation

$$T = \frac{R_{in}}{R_{out}} = \exp(-nl\sigma_{tot}) \ , \tag{1}$$

$$\sigma_{tot} = -\frac{1}{nl}\ln\left(\frac{R_{in}}{R_{out}}\right) = -\frac{1}{nl}\ln(T) \ , \tag{2}$$

where R_{in} , R_{out} are the background and dead-time corrected count rates in the detector with the sample in and out of the beam, respectively. The areal density *nl* is given by the product of the number density of atoms and the thickness and σ_{tot} is the neutron total cross section. The Au and Ta samples used are characterized in Table 1. The areal density *nl* is known to a relative uncertainty of $6 \cdot 10^{-3}$.

The spectra of transmitted neutrons measured as a function of time-of-flight are shown in Fig. 2. The flight path from the centre of the neutron radiator to the centre of the plastic scintillator was determined by geometrical survey to be 717.5 ± 0.2 cm. The bremsstrahlung peak from the neutron radiator has a time-of-flight of 23.9 ns. The fastest neutrons arrive at about 100 ns after this peak. Measurements with a ^{235}U fission chamber, which is sensitive down to the thermal region, show that the neutron energy range extends down to about 10 keV [12].

Table 1: Ta and Au sample characteristics. The samples had cylindrical shape. The density has been calculated from the measured dimensions and mass of the sample to show agreement with the standard density within the relative uncertainty of $6 \cdot 10^{-3}$ or better. The Ta corresponds to ASTM B365 Grade RO5200, the gold to standard fine gold. The bremsstrahlung absorbers consisted of technical lead alloy (PbSb4) machined to a cylinder (diameter 25.0±0.1 mm, length 30.0±0.1mm).

Sample	**Diameter (mm)**	**Length (mm)**	**Mass (g)**	**Density (g/cm^3)**	**Standard Density (g/cm^3)**	**Purity (weight %)**	**Areal Density *nl* (atoms/barn)**
Ta	25.1±0.1	25.5±0.1	210.419±0.001	16.68±0.09	16.65	99.95	0.1413±0.0006
Au	26.0±0.1	16.0±0.1	163.760±0.001	19.28±0.12	19.32	99.99	0.0945±0.0006

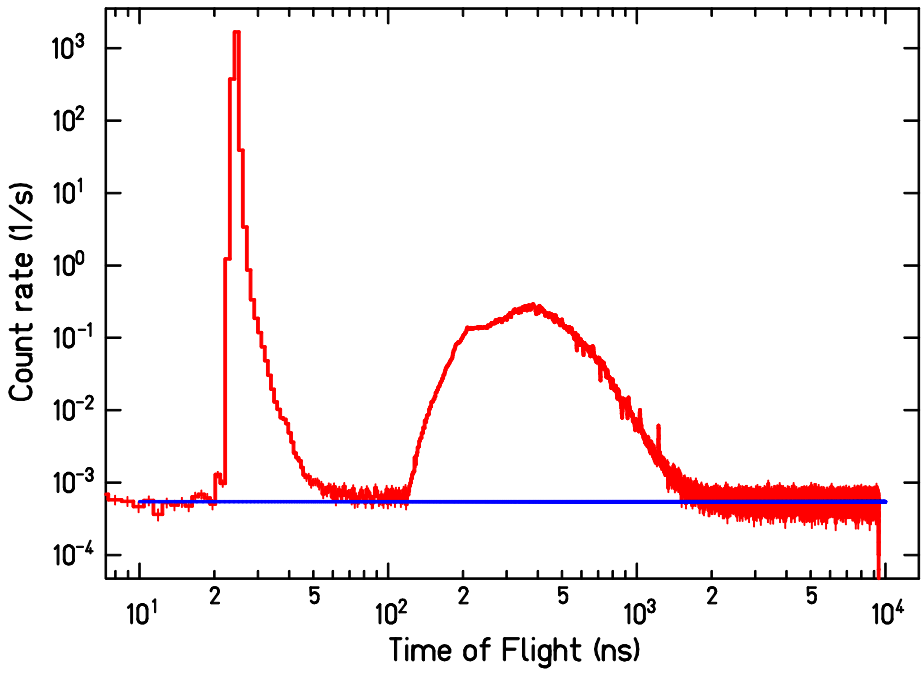

Fig. 2: Typical time-of-flight spectrum for the transmission measurement at nELBE. The dead-time corrected count rate is shown as a function of time-of-flight for the transmission through the Au sample + Pb absorber. A narrow gate was set on the time difference of the two PMTs to select the region, where the transmitted neutron beam passes through the scintillator. The random background rate (blue line) was fitted in the time interval from 8500 ns – 9350 ns. The time resolution of the detection system is characterized by the width of the bremsstrahlung peak and amounts to 0.46 ns.

4 Data analysis and experimental uncertainties

To determine the neutron transmission and the total cross section from the measured time-of-flight distribution several corrections have to be done:

1. Correction for a time-of-flight dependent dead time
2. Subtraction of a constant random background in the time-of-flight spectra
3. Neutron beam intensity fluctuations
4. In-scattering of neutrons
5. Resonant self shielding in thick transmission samples

Random background and dead-time corrections are very important. The remaining neutron beam intensity fluctuations were measured in the target cycle and found to have a small influence. In-scattering of neutrons was minimized by using a "good" geometry. Resonant self shielding can be an important correction at low neutron energy, where the total cross section can have strong, separated resonances [9]. Above 100 keV neutron energy this correction is found to be negligible.

A detailed discussion of all corrections as well of the energy resolution and the uncertainty budget can be found in Ref. [1].

5 Results

The neutron total cross sections of Ta and Au have been measured in the energy range from about 0.1 MeV to 10 MeV. The energy resolution $\Delta E/E$ over this energy range increases from 1.4 % to 7.4 % (FWHM). The energy resolution is mostly due to the scattering of neutrons in the lead shield of the plastic scintillator. The resolution is sufficient for average cross sections that can be compared with optical model calculations.

In Fig. 3 the neutron total cross section of Au is shown in comparison with the data from Poenitz *et al.* [9, 16] and Abfalterer *et al.* [8]. The nELBE data are systematically about 2 % higher than the other two experiments. The typical statistical uncertainty is smaller than 5 % for Au data at 100 keV and above as was asked for in the High Priority Request List of the Nuclear Energy Agency [4]. Also our measurement extends up to the very accurate data of Abfalterer *et al.* [8] and thus demonstrates good consistency. The calculated total cross section of the Talys 1.4 reaction code [17] shows good agreement with the data to within 4 %. The Talys code was used with the default options, using the optical model parameters from Koning and Delaroche [2]. Concerning the neutron total cross section of ^{197}Au all current evaluations are quite similar. The JEFF-3.1.2 and CENDL-3.1 evaluations are about 2-3 % lower than the experimental data. The corresponding ENDF/B-VI.8, ENDF/B-VII.0, and ENDF/B-VII.1 evaluations are identical to JEFF-3.1.2. The JENDL-4.0 evaluation is up to 5 % higher than the evaluations mentioned before.

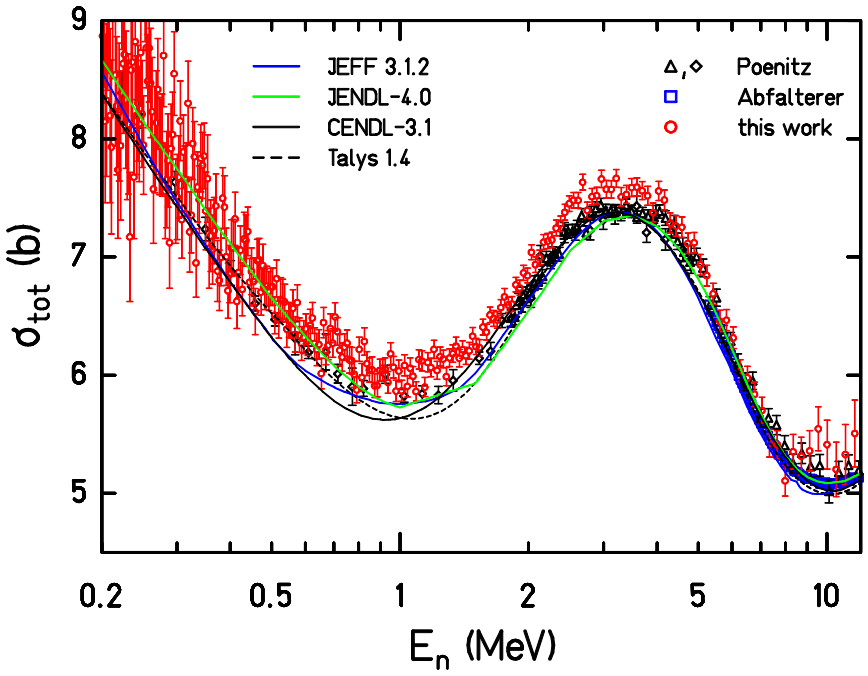

Fig. 3: The experimental neutron total cross section of ^{197}Au as a function of the neutron energy from 0.2 MeV to 10 MeV (this work, red circles). The data from Abfalterer *et al.* [8] from the LANL WNR spallation neutron source are shown as blue squares. The black symbols denote results from Poenitz *et al.* [9, 16] from the ANL fast neutron generator. The nELBE data have an equidistant binning in time of 3.9 ns to decrease statistical uncertainties and to increase the readability of the figure. The dashed line shows a result from the Talys code [17]. The JEFF-3.1.2 evaluation is shown by a blue line. The JENDL-4.0 evaluation is shown as a green line and the CENDL-3.1 evaluation as a black line.

Figure 4 shows the neutron total cross section of Ta. In the energy range from 0.2 MeV to 10 MeV our data are about 3 % higher than results from Finlay *et al.* [7] and Poenitz *et al.* [9, 16] that covered only a part of this energy range. Older data by A.B. Smith [18] are very close in the absolute normalization. A small gap from 0.6 MeV to 1.0 MeV where no high resolution data existed before has been filled. The Talys 1.4 reaction code does not describe the neutron total cross section correctly in the energy range below 2 MeV.

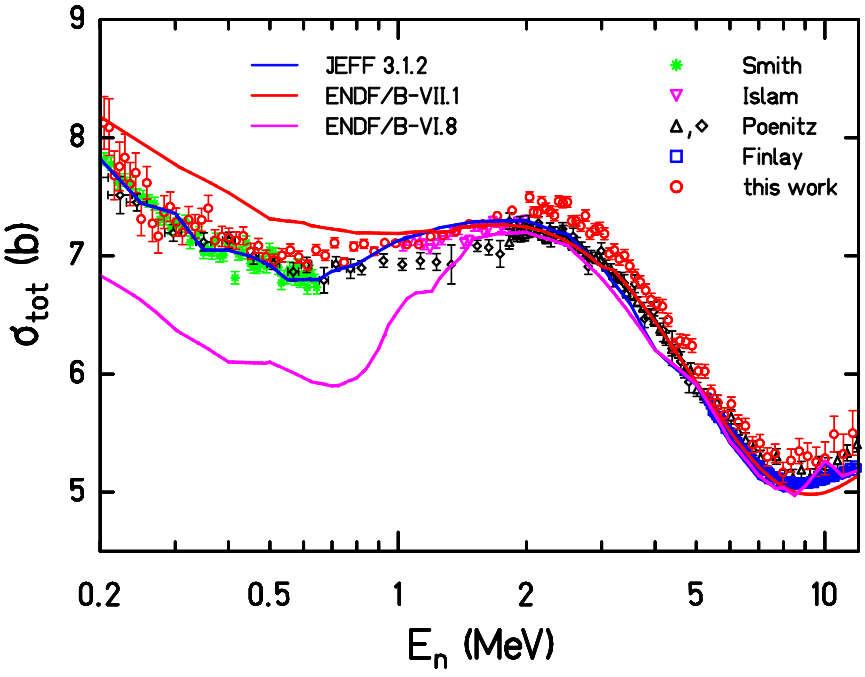

Fig. 4: The neutron total cross section for ^{nat}Ta as a function of the neutron energy from 0.2 MeV to 10 MeV (this work, red circles). The data from Finlay *et al.* [7] at the LANL WNR spallation neutron source are shown as blue squares. The black symbols denote results from Poenitz *et al.* [9, 16] from the ANL fast neutron generator. The green and purple symbols denote data from Refs. [18] and [19], respectively. The ENDF/B-VII.1 evaluation is shown by a red curve; the ENDF/B VI.8 evaluation by a purple line. The JEFF-3.1.2 evaluation is shown by a blue line. The experimental data of Refs. [18, 19] and this work below 2 MeV have been rebinned to increase readability.

The neutron total cross section of Ta is also compared to different recent nuclear data evaluations in Fig. 4. The JEFF-3.1.2 evaluation is in good agreement with the experimental data, as are the nearly identical curves from RUSFOND 2010 and JENDL-4.0. The ENDF/B-VI.8 and the identical ENDF/B-VII.0 evaluations are below the data. The ENDF/B-VII.1 evaluation is above the data in the energy range below 1 MeV. These discrepancies show again the importance of neutron-total cross section measurements in the fast-energy range covered in this work. This work allows us to base nuclear data evaluations on experimental neutron total cross sections in the energy range below 5 MeV, which is especially sensitive on the optical model parameters used. A careful measurement as recommended in [6] has been done.

Additional figures of the measured neutron total cross sections of ^{197}Au and ^{nat}Ta with different binning or in a different energy range can be found in Ref. [1].

The present results with a systematic uncertainty of 1 % might be an indication that the total cross section could be slightly higher than the ones measured before at LANL and ANL. Our detection system had a low detection threshold and good efficiency; however the PMT afterpulsing caused high single count rates that cause additional dead time. To investigate systematic uncertainties in future transmission measurements a data acquisition with much smaller

dead-time correction is in preparation. The data measured in this work will be made available through the EXFOR data base. A table of cross sections has been added as electronic supplementary material to Ref. [1].

An improved time-of-flight facility is currently under construction in the National Center for High Power Radiation Sources of HZDR Dresden, which includes a 6 m x 6 m x 9 m time-of-flight hall with reduced background from scattering on the walls. This facility will also allow improved measurements of neutron total cross sections to assist future nuclear data evaluations [20].

Acknowledgement

We thank Andreas Hartmann for technical support and preparation of the experiments and the ELBE accelerator crew for providing very stable beam operation. This work is supported by the German Federal Ministry for Education and Science (TRAKULA project, contract number 02NUK13A) and by the European Commission in the projects EFNUDAT (FP6-036434) and ERINDA (FP7-269499).

References

[1] R. Hannaske *et al*., *Eur. Phys. J.* **A 49** (2013) 137.

[2] A. Koning and J. Delaroche, *Nucl. Phys.* **A 713** (2003) 231.

[3] P. Pereslavtsev and U. Fischer, *Nucl. Inst. Meth.* **B 248** (2006) 225.

[4] NEA Nuclear Data High Priority Request List (HPRL)
Available online: http://www.oecd-nea.org/dbdata/hprl/hprlview.pl?ID=428.

[5] R.L. Klueh, Oak Ridge National Laboratory Report (2004) ORNL/TM-2004/176.

[6] A.B. Smith, *Ann. Nucl. Ene.* **32** (2005) 1926.

[7] R.W. Finlay *et al*., *Phys. Rev.* **C 47** (1993) 237.

[8] W.P. Abfalterer *et al*., *Phys. Rev.* **C 63** (2001) 044608.

[9] W. Poenitz, J. Whalen and A. Smith, *Nucl. Sci. Eng.* **78** (1981) 333.

[10] I. Sirakov *et al.*, *Eur. Phys. J.* **A 49** (2013) 144.

[11] J. Klug *et al*., *Nucl. Inst. Meth.* **A 577** (2007) 641.

[12] R. Beyer *et al*., *Nucl. Inst. Meth.* **A 723** (2013) 151.

[13] E. Altstadt *et al*., *Ann. Nucl. Ene.* **34** (2007) 36.

[14] F. Gabriel *et al*., *Nucl. Inst. Meth.* **B 161** (2000) 1143.

[15] R. Beyer *et al*., *Nucl. Inst. Meth.* **A 575** (2007) 449.

[16] W. Poenitz and J. Whalen, Argonne National Laboratory (1983) ANL/NDM-80.

[17] A. Koning, S. Hilaire and M. Duijvestijn, Proc. Int. Conf. Nucl. Data Science and Tech., April 22-27, 2007 Nice, France, EDP Sciences (2008) 211.

[18] A.B. Smith, P.T. Guenther and J.F. Whalen, *Phys. Rev.* **168** (1968) 1344.

[19] E. Islam *et al*., *Nucl. Phys.* **A 209** (1973) 189.

[20] A.R. Junghans, Proc. Int. Conf. Nucl. Data Science and Tech., New York, 2013,
to be published in *Nucl. Data Sheets* (2014).